

Article

Study on the Effect of External Air Supply and Temperature Control on Coal Spontaneous Combustion Characteristics

Changkui Lei ^{1,*}, Xueqiang Shi ^{2,*}, Lijuan Jiang ³, Cunbao Deng ¹, Jun Nian ¹ and Yabin Gao ¹

¹ College of Safety and Emergency Management Engineering, Taiyuan University of Technology, Taiyuan 030024, China

² School of Environment and Safety Engineering, North University of China, Taiyuan 030051, China

³ Faculty of Business and Economics, University of Pécs, 7626 Pécs, Hungary

* Correspondence: leichangkui@tyut.edu.cn (C.L.); shixueqiang@nuc.edu.cn (X.S.)

Abstract: Coal spontaneous combustion in underground mine goaf has a great impact on coal mining. The temperature-programmed experiment is a commonly used and effective method for studying the characteristics of coal spontaneous combustion. Aiming at the problem that the numerical simulation of coal spontaneous combustion characteristics under the condition of external air supply and temperature control in a temperature-programmed experiment is insufficient, a multi-physical field coupling numerical model of coal spontaneous combustion in the temperature-programmed experiment is established. The variation characteristics of coal temperature, oxygen, and oxidation products under external air supply and temperature control were studied. The results show that the numerical simulation results are consistent with the experimental results. With the increase in temperature, the volume fractions of oxygen and carbon dioxide decrease and increase, respectively. As the air supply volume increases, the oxygen volume fraction at the outlet increases, and the peak value of the oxygen volume fraction change rate exhibits a “hysteresis” feature, and the time corresponding to the peak value increases. Moreover, the temperature change rate increases. With the increase in the heating rate, the peak value of the oxygen volume fraction change rate increases and shows an “early appearance” characteristic, at the same time, the maximum coal temperature displays a linear increase trend.

Keywords: coal spontaneous combustion; air supply volume; heating rate; oxygen volume fraction; numerical simulation



Citation: Lei, C.; Shi, X.; Jiang, L.; Deng, C.; Nian, J.; Gao, Y. Study on the Effect of External Air Supply and Temperature Control on Coal Spontaneous Combustion Characteristics. *Sustainability* **2023**, *15*, 8286. <https://doi.org/10.3390/su15108286>

Academic Editors: Baoqing Li, Xiangguo Kong, Dexing Li and Xiaoran Wang

Received: 6 March 2023

Revised: 14 April 2023

Accepted: 12 May 2023

Published: 19 May 2023



Copyright: © 2023 by the authors. Licensee MDPI, Basel, Switzerland. This article is an open access article distributed under the terms and conditions of the Creative Commons Attribution (CC BY) license (<https://creativecommons.org/licenses/by/4.0/>).

1. Introduction

Coal spontaneous combustion is one of the main disasters that affect coal mine safety [1]. It not only causes resource waste and equipment damage but also leads to gas and coal dust explosions, triggering secondary disasters and causing serious casualties and property losses [2]. Due to the concealment and difficulty in accessing the interior of the goaf, it is one of the most prone locations for coal spontaneous combustion [3,4]. Once the conditions of oxidation reaction are met, namely, oxygen and a good thermal storage environment, coal will spontaneously undergo an exothermic reaction, and the temperature rise of coal caused by the oxidation reaction will feedback to accelerate its reaction process, eventually achieving extremely hazardous and violent combustion [5,6]. Therefore, the problem of coal spontaneous combustion in goaf has always been an urgent problem that troubles the safety production of mines [7]. However, in the actual production process of mines, avoiding oxidation reactions of residual coal in goaf is the key to preventing coal spontaneous combustion, which mainly involves analyzing the environment of coal spontaneous combustion in goaf. Therefore, coal spontaneous combustion and its influencing factors are one of the important topics of fire science research [8,9]. By investigating the characteristics of coal spontaneous combustion under different environmental conditions, it is possible to have a more comprehensive understanding of the oxidation laws of coal

spontaneous combustion, which has important guiding significance for the prevention and control of coal spontaneous combustion in goaf.

In view of the coal oxidation reaction and its characteristics, a lot of studies have been conducted in recent years, including the use of advanced experimental instruments and self-developed equipment to study the mechanism and characteristics of its spontaneous combustion [10–12]. Deng et al. [13] tested the heat release intensity and oxygen consumption rate of the coal samples with a temperature-programmed device and calculated the change law of gas products of coal spontaneous combustion. Qi et al. [14] built a similar experimental platform for coal smoldering simulation and studied the smoldering characteristics of coal fire under different air supply rates. Wen et al. [15] compared and analyzed the characterization parameters of coal spontaneous combustion through two different experimental systems, the large-scale coal spontaneous combustion experiment, and the isothermal difference leading experiment. Beamish et al. [16] studied the influence of moisture content, initial temperature, coalbed methane content, and reactive pyrite content on the self-heating rate of low-temperature coal through an adiabatic furnace test. Further, Zhang et al. [17] established a calculation method for the coal spontaneous combustion period based on pure oxygen adiabatic oxidation experiment. Jia et al. [18] employed the temperature-programmed experimental system to conduct oxidation experiments on coal samples with six oxygen concentrations and studied the gas products of coal samples at different temperature stages.

In addition, with the development of computing technology, numerical simulation has gradually become an effective means to predict the risk of coal spontaneous combustion and optimize industrial conditions [19,20]. Meanwhile, it also provides a reliable method for studying the coal spontaneous combustion process and external coal spontaneous combustion conditions in goaf [21,22]. Shi et al. [23] used numerical simulation and experimental methods to explore the characteristics of temperature evolution in large coal spontaneous combustion silo and obtained the movement law of high temperature points. Li et al. [24] adopted numerical simulation to study the compound hazard area of coal spontaneous combustion and gas and obtained the change characteristics of the hazard area under the change of relevant parameters. Ma et al. [25] studied the distribution of oxygen concentration in adjacent goafs by numerical simulation method and determined the risk zone of spontaneous combustion in adjacent goafs. Yuan et al. [26] adopted the obtained experimental data to simulate the oxidation and temperature rise process of different coal samples in the longwall goaf with three-dimensional CFD, and studied the influence of coal surface area and reaction heat on the natural heat release process. Liu et al. [27] developed a new transient model under the framework of multi-physical coupling to simulate the process of coal spontaneous combustion during stopping mining in longwall goaf.

However, there are few studies on the influence of external conditions, especially external air supply, temperature control, etc. on coal spontaneous combustion characteristics. Ren et al. [28] used a C80 experimental system to study the low-temperature oxidation heat flux of pulverized coal under different oxygen concentrations to investigate the risk of spontaneous combustion of pulverized coal. Yan et al. [29] conducted a programmed temperature rise experiment to test the oxidation process of coal samples at different oxygen concentrations. Therefore, current research on the impact of the external environment on coal spontaneous combustion mainly focuses on controlling oxygen concentration, rather than directly regulating the gas supply. In addition, the analysis of the impact of temperature control on coal spontaneous combustion is mainly reflected in the analysis of the heating rate on the thermal kinetics of coal oxidation. For example, Zhang et al. [30] studied the thermodynamic parameters of coal spontaneous combustion at different heating rates before and after the ignition temperature. Sabat et al. [31] studied the thermal degradation characteristics, kinetics, and thermodynamics of different grades of low-rank coal at different heating rates through thermogravimetric analysis. Meanwhile, Wang et al. [32] employed a thermogravimetric simulation test bench to study the pyrolysis characteristics and kinetics of bituminous coal at different heating rates.

In this paper, the characteristics of coal spontaneous combustion under different external air supplies and temperature controls are studied by using a numerical simulation method combined with a self-developed temperature-programmed coal spontaneous combustion experiment. The characteristics of reactants, products, and temperature changes during the coal oxidation reaction were obtained. This study is of great significance for understanding the characteristics of coal spontaneous combustion and preventing its occurrence in goaf.

2. Experiment and Methodology

2.1. Coal Sample

To study the oxidation process of coal spontaneous combustion, lignite from the Wantugou coal mine, in Shaanxi Province, China, was used as the experimental coal sample. Fresh coal samples are collected from the in situ and transported to the laboratory through oxygen isolation. After being crushed by a jaw crusher, coal samples with a particle size of 3–5 mm are screened out as experimental samples. For the experiment, 1 kg coal samples with the same particle size range were selected. Table 1 shows the results of proximate and element analyses of the coal sample.

Table 1. The proximate and element analyses of coal sample.

Proximate Analysis				Ultimate Analysis				
$M_{ad}/\%$	$V_{ad}/\%$	$A_{ad}/\%$	$FC_{ad}/\%$	$C_{daf}/\%$	$H_{daf}/\%$	$O_{daf}/\%$	$N_{daf}/\%$	$S_{daf}/\%$
11.75	35.78	13.03	39.44	65.36	1.25	12.66	1.91	0.52

Note: M_{ad} , V_{ad} , A_{ad} , and FC_{ad} correspond to air-dried moisture, volatile matter, ash, and fixed carbon, respectively; C_{daf} , H_{daf} , O_{daf} , N_{daf} , and S_{daf} correspond to dry ash-free carbon, hydrogen, oxygen, nitrogen, and sulfur, respectively.

2.2. Experiment

The experimental equipment is a self-developed temperature-programmed device that leads the oxidation reaction of coal under additional heating conditions. Figure 1 presents the schematic diagram of the temperature-programmed system used in the experiment, which includes three parts, namely the gas supply system, the temperature control system, and the gas analysis system.

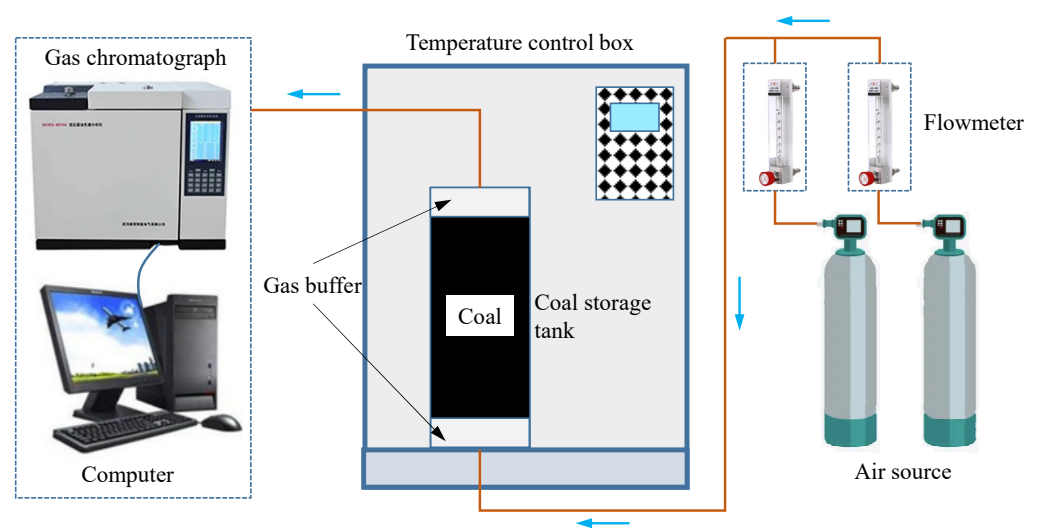


Figure 1. Schematic diagram of the temperature-programmed experiment system.

To prevent heat loss and maintain constant heating conditions, the coal storage tank is placed in the temperature-programmed heating box. The temperature-programmed heating box is automatically controlled by a silicon-controlled regulator with a furnace

space of $50 \times 40 \times 30$ cm. The sample tank for coal storage is made of stainless steel, with a height and radius of 220 mm and 50 mm, respectively. To obtain a more uniform oxygen supply environment, 20 mm gas buffer space is set at the upper and lower parts of the coal storage tank. In the experiment, nitrogen and oxygen were premixed at 79:21 to simulate the air environment. In order to keep the intake temperature basically the same as the temperature of the coal sample, a 2 m long copper tube is coiled in the temperature-programmed heating box, and the air flow is preheated through the coil before entering the coal sample.

Before the experiment, the coal storage tank was continuously ventilated for half an hour to ensure that the gas in the coal storage tank is constant, and the gas entering the coal storage tank was controlled by the flow control valve and float flowmeter. In addition, in order to ensure that the difference in oxygen concentration between the inlet and outlet of the coal sample tank can be within the resolution range of the gas chromatograph used in mining, the experimental gas supply flow rate should be 41.8–190.0 mL/min. Therefore, the experimental gas supply flow rate is set to 120 mL/min, and the test is stopped after the coal is heated to 180 °C at a heating rate of 0.3 °C/min. The gas produced in the experiment was analyzed by the SP-2120 gas chromatograph. K-type thermocouples are set at the center of the coal body and the wall of the coal storage tank to measure the temperature.

2.3. Numerical Model

Coal oxidation reaction involves multiple physical processes, such as fluid flow, heat transfer, mass transfer, and chemical reaction. To solve the parameter coupling law of multiple physical fields, the multi-physical field coupling software COMSOL Multiphysics (COMSOL, Stockholm, Sweden) was applied to solve the reaction process. According to the actual experimental conditions, the numerical model of programmed temperature rise of coal spontaneous combustion is established considering the momentum, mass, energy transfer, and chemical reaction process. For the heat transfer during coal oxidation and heating, the energy equation is as follows [33,34]:

$$(\rho C_p)_{\text{eff}} \frac{\partial T}{\partial t} + \rho C_p \vec{u} \cdot \nabla T + \nabla \cdot \vec{q} = Q \quad (1)$$

where ρ is the density of gas, kg/m^3 ; C_p is the specific heat of gas at constant pressure, $C_p = 2.8 T + 50$ according to the experiment, $\text{J/kg}\cdot\text{K}$; $(\rho C_p)_{\text{eff}}$ is the average effective volume heat capacity at atmospheric pressure considering the characteristics of solids and gases, $\text{J/m}^3\cdot\text{K}$; T is the temperature, K ; \vec{q} is heat conduction flux, W/m^2 ; \vec{u} is the velocity vector, m/s ; and t is time, s .

The Brinkman equation is employed to solve the fluid flow in the coal void [35,36]:

$$(1 - \varepsilon) \frac{\partial \rho_c}{\partial t} = -V_c \quad (2)$$

$$\frac{\partial \varepsilon \rho}{\partial t} + \nabla \cdot (\rho \vec{u}) = Q_{br} \quad (3)$$

$$\rho \frac{\partial \vec{u}}{\partial t} = \nabla \cdot [-p \vec{I} + \mu \frac{1}{\varepsilon} (\nabla \vec{u} + (\nabla \vec{u})^T) - \frac{2}{3} \mu \frac{1}{\varepsilon} (\nabla \cdot \vec{u}) \vec{I}] - \frac{Q_{br}}{\varepsilon^2} \vec{u} \quad (4)$$

where ε is the porosity of the coal sample; ρ_c is the density of the coal sample, kg/m^3 ; V_c is the coal oxidation reaction rate, $\text{kg/m}^3\cdot\text{s}$; Q_{br} is the mass source, $\text{kg/m}^3\cdot\text{s}$; and μ and p are dynamic viscosity and pressure, respectively, $\text{kg/m}\cdot\text{s}$, Pa .

Considering the generation and consumption of various substances in the coal oxidation process, Equation (5) is used to solve for the material transfer:

$$\frac{\partial(\varepsilon c_j)}{\partial t} + \nabla \cdot \vec{J}_j + \vec{u} \cdot \nabla c_j = V_j \quad (5)$$

where \vec{J}_j is mass flux, $\text{kg}/\text{m}^2\cdot\text{s}$; c_j represents gas concentration, mol/m^3 ; and the subscript j indicates the type of gas.

Table 2 provides the parameter values that need to be assigned to the numerical model mentioned above. Based on the actual situation on site and corresponding thermophysical experiments, the physical parameters of coal were obtained, and it is assumed that the parameters in the table are fixed values and do not change with temperature and other conditions.

Table 2. Physical parameters used in numerical simulation.

Parameters	Description	Value
p_0	Pressure (atm)	1
T_0	Initial temperature ($^{\circ}\text{C}$)	30
R_s	Specific gas constant ($\text{J}/\text{kg}\cdot\text{K}$)	287
γ	Specific heat	1.4
k_c	Thermal conductivity ($\text{W}/\text{m}\cdot\text{K}$)	0.21
ρ_c	Coal density (kg/m^3)	1200
$C_{p,c}$	Specific heat capacity ($\text{J}/\text{kg}\cdot\text{K}$)	1000

3. Results and Discussion

3.1. Numerical Simulation Verification

To verify the reliability of the numerical simulation method, the simulation results and experimental data are compared and analyzed. Figure 2 shows the changes in oxygen and carbon dioxide volume fraction with temperature under the condition that the initial and boundary conditions of the numerical simulation are consistent with those of the experiment. By comparing the simulation results of oxygen and carbon dioxide volume fractions with the experimental results, it is found that the average error is 2.3% and 4.6%, respectively. Thus, the results of the experiment and simulation are in good agreement, which demonstrates that the acquisition of numerical simulation parameters and the numerical simulation method can reasonably characterize the coal oxidation and heating process. In addition, with the increase in coal temperature, the oxygen volume fraction at the outlet gradually decreases and the carbon dioxide volume fraction gradually increases, which indicates that the oxygen consumption gradually increases with the increase in temperature [37].

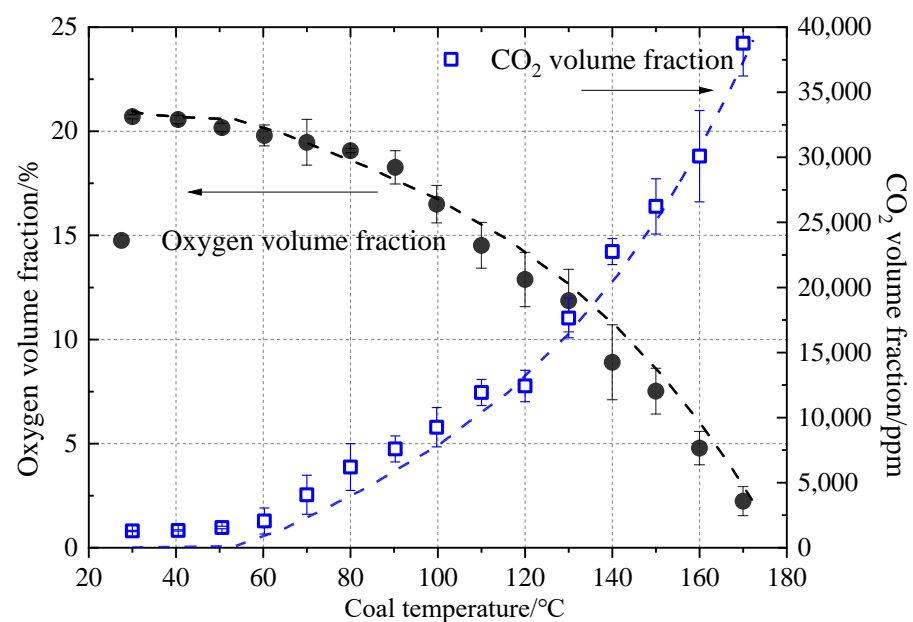


Figure 2. Changes of oxygen and carbon dioxide at the outlet with temperature during coal oxidation.

3.2. Influence of Inlet Air Volume on Coal Spontaneous Combustion Characteristics

As is well known, air leakage in the working face has a significant impact on the spontaneous combustion of coal in the goaf and is the main cause of coal spontaneous combustion in the goaf [38]. To further study the influence of inlet air volume on the coal spontaneous combustion process, the inlet air volume was changed in the numerical simulation, and the programmed heating rate was set to $0.375\text{ }^{\circ}\text{C}/\text{min}$. Figure 3 shows the oxygen volume fraction and its change rate at the outlet under different air volume conditions. As can be seen from Figure 3a, with the increase in air supply, the oxygen volume fraction at the outlet also shows an increasing trend, which is due to the slow oxidation reaction of coal at low temperature and the small consumption of oxygen. Take the fourth hour as an example, the oxygen gas integral value at $144\text{ mL}/\text{min}$ is 1.77 times higher than that without ventilation. Figure 3b shows that the peak value of the oxygen volume fraction change rate at the outlet is “hysteresis” with the increase in air volume. The “hysteresis” feature is that the increase in air supply promotes the heat loss inside the coal body, and the peak value of the coal oxidation reaction is delayed. The above results prove that heat is the main factor that dominates the reaction of coal at the initial stage of low-temperature oxidation [39].

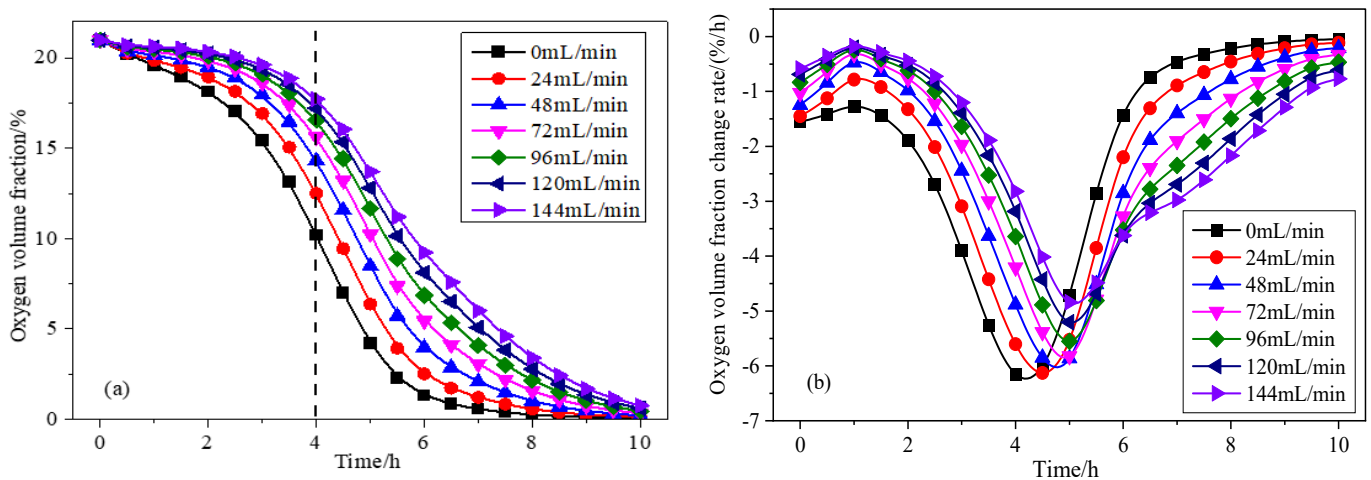


Figure 3. Oxygen volume fraction and its change rate at the outlet under different air volumes: (a) oxygen volume fraction; (b) oxygen volume fraction change rate.

Figure 4 gives the relationship between the peak time of the oxygen volume fraction change rate at the outlet and the flow rate. With the increase in flow rate, the peak time of the change rate increases. Further, based on the method of numerical fitting, Equation (6) shows the relationship between them.

$$y = -1.36e^{-x/64} + 5.38 \quad (6)$$

With the further increase in the flow rate, it can be predicted that the peak time of the change rate will not change, which highlights the leading role of oxygen, that is, under a certain low-temperature oxidation rate of coal, temperature dominance will change to oxygen dominance.

Figure 5 shows the maximum coal temperature and its change rate under different air supply conditions. It can be seen from Figure 5a that the maximum coal temperature before 7.5 h is always lower than the leading temperature of programmed temperature rise. Except for air volume of 0 and 24 mL/min, the maximum coal temperature under other air supply conditions exceeds the leading temperature of programmed temperature rise after 7.5 h. This shows that the oxidation reaction of coal after 7.5 h is the main reason for the temperature increase, and sufficient oxygen supply promotes the rapid coal oxidation

reaction, while the heat release of coal oxidation at air volume of 0 and 24 mL/min is less than the heat dissipation, so their heat cannot be accumulated.

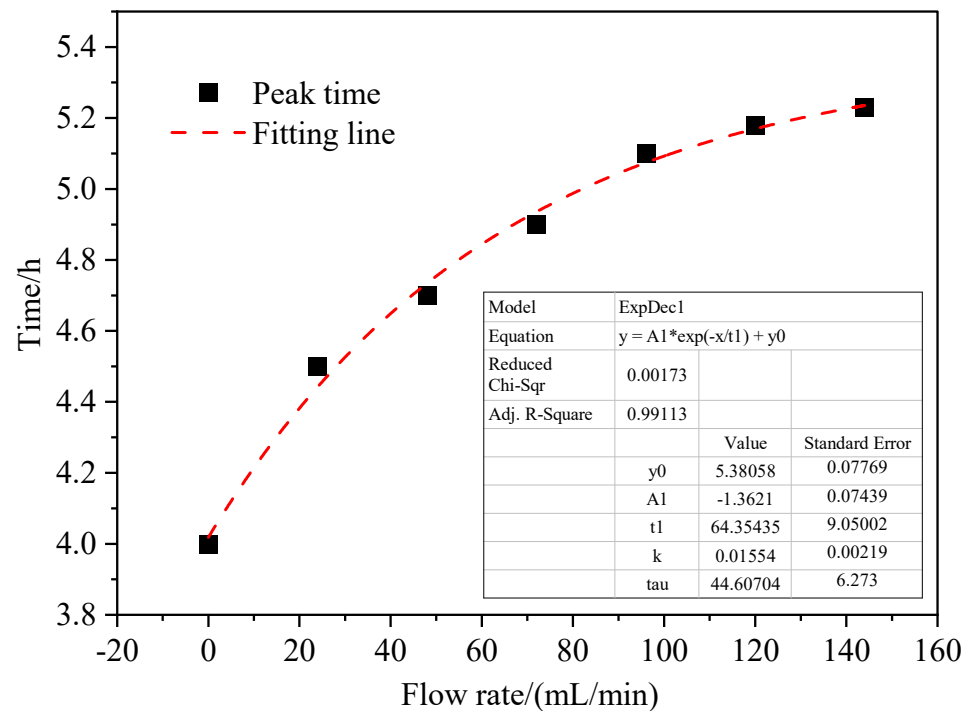


Figure 4. The relationship between the peak time of oxygen volume fraction change rate at the outlet and flow rate.

From Figure 5b, it can be seen that except for the air volume of 0 and 24 mL/min, the maximum temperature change rate of coal under other air supply conditions exceeds the temperature change rate adjusted by the programmed temperature rise system within 4 h, and as time goes on, the larger the air supply volume is, the more obvious the increase is. This reflects that after 4 h, the oxidation heat release of coal is greater than the heat dissipation, resulting in heat accumulation. Furthermore, it also shows that the greater the air supply, the more intense the chemical reaction of the spontaneous oxidation process of coal, and the greater the heat production. However, the oxidation heat release of the coal sample at air volume of 0 and 24 mL/min is lower, and its temperature change rate changes slightly with the increase in time, which is mainly due to the insufficient air supply and the inability to provide sufficient oxygen for the coal oxidation reaction. Therefore, oxygen conditions are a key factor in the occurrence of coal spontaneous combustion [40,41]. Only by minimizing air leakage and oxygen supply in the goaf can we prevent the occurrence of coal spontaneous combustion in the goaf.

In order to more intuitively reflect the relationship between coal spontaneous combustion temperature and air supply flow, Figure 6 shows the maximum coal temperature at 10 h under different air supply conditions. The maximum coal temperature under the condition of air volume of 0 and 24 mL/min is lower than the leading temperature of programmed temperature rise. With the increase in air supply volume, the maximum coal temperature shows an upward trend, and the two are positively correlated as a whole. Equation (7) is obtained by linear fitting of the maximum coal temperature at 10 h with different air supply conditions.

$$y = 0.675x + 288 \quad (7)$$

When the air volume is less than 24 mL/min, the result does not conform to a linear change. The air volume exceeds 24 mL/min, and the result conforms to the characteristics of linear change. The internal reason for this different trend is that the oxygen content

determines the completeness of the coal oxidation reaction. Therefore, in the process of prevention and control of coal spontaneous combustion in the mine goaf, the control of air leakage in the goaf is crucial, which is the key measure to prevent the occurrence of coal spontaneous combustion [42].

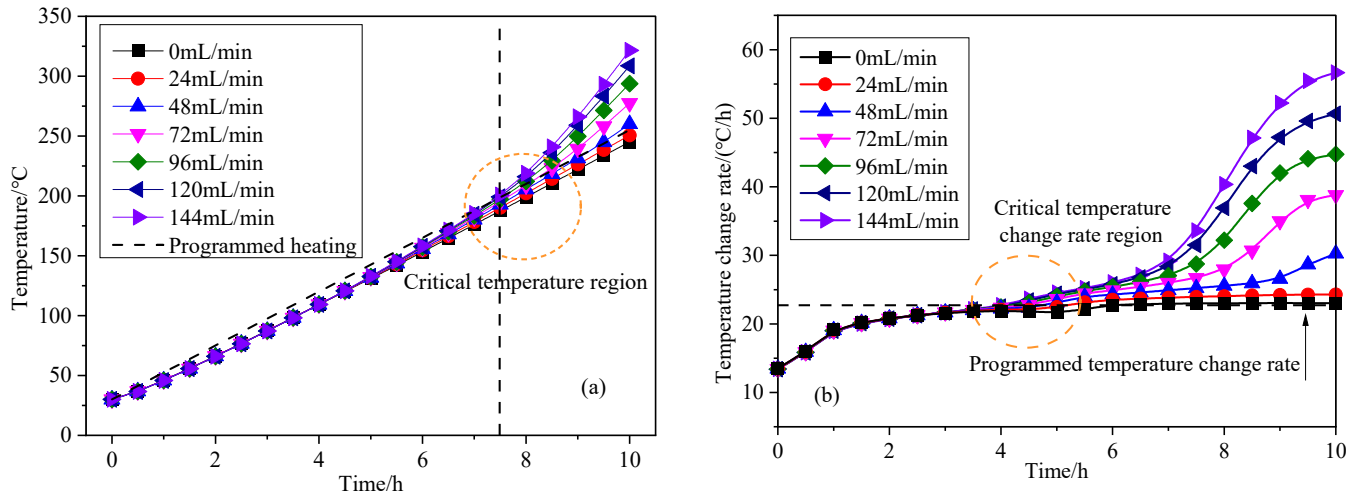


Figure 5. Maximum coal temperature and its change rate under different air supply conditions: (a) coal temperature; (b) coal temperature change rate.

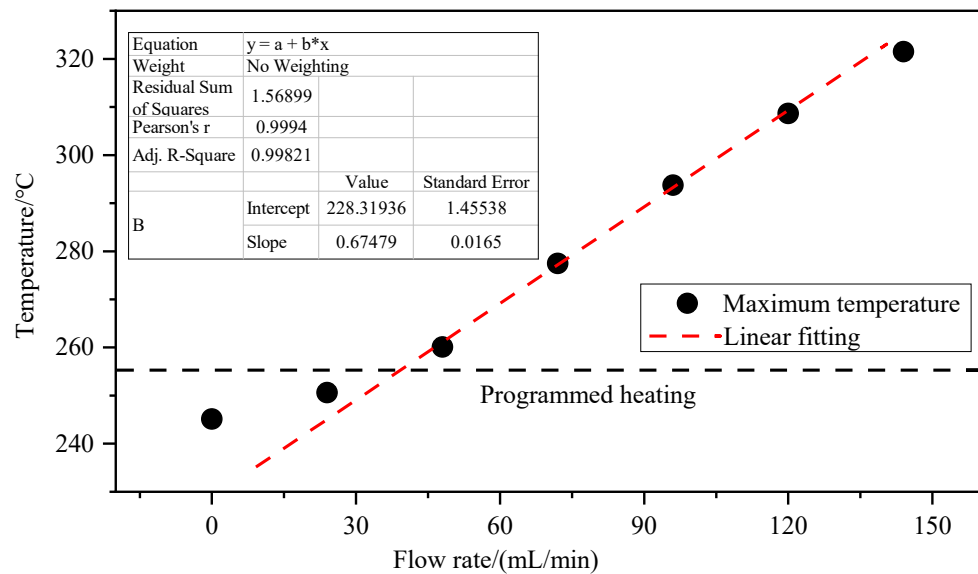


Figure 6. Maximum coal temperature at 10 h under different air supply conditions.

Figure 7 displays the cloud diagram of oxygen volume fraction and temperature distribution under different air flow conditions at the 10th hour. With the increase in air flow, the area with high oxygen volume fraction moves upward, for example, the line representing 1% oxygen volume fraction moves upward, as shown in Figure 7a. The distribution of oxygen volume fraction reflects that with the migration of oxygen in coal, oxygen is consumed due to the low-temperature oxidation reaction of coal. Obviously, the higher the air flow, the higher the oxygen volume fraction in the coal body. The distribution of oxygen volume fraction in the coal body presents stratified characteristics.

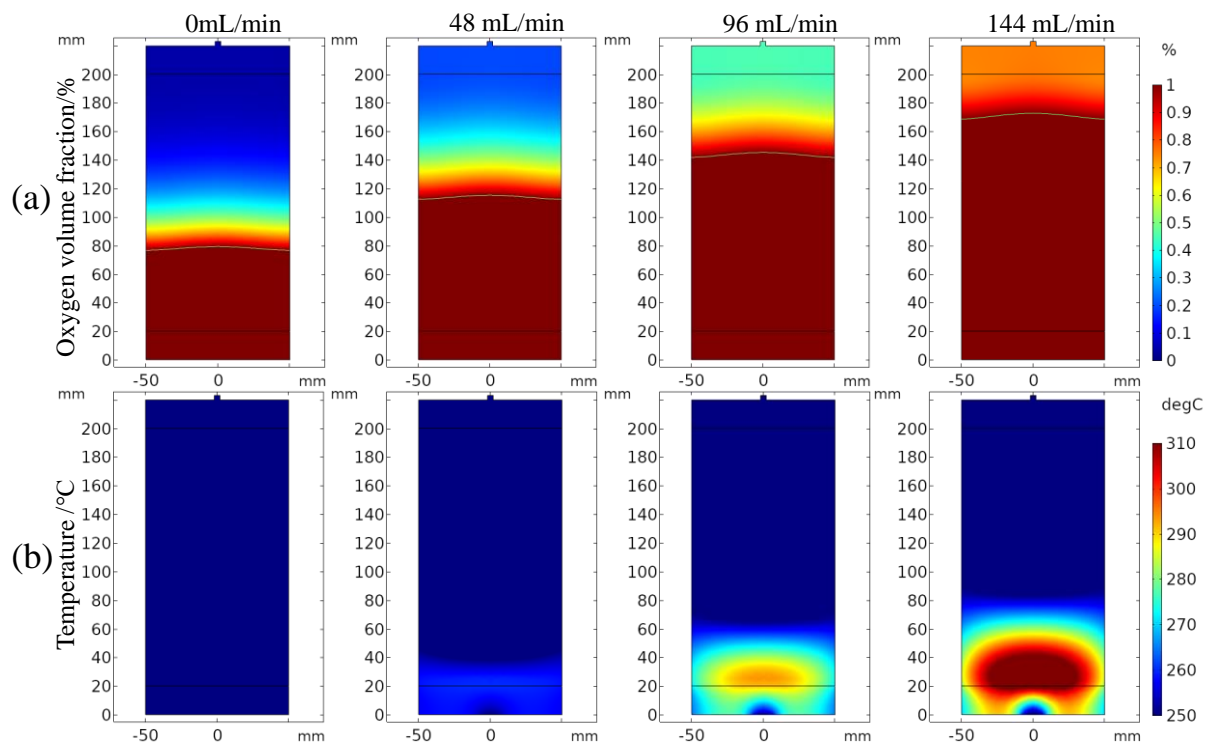


Figure 7. Cloud diagram of oxygen volume fraction and temperature distribution under different air flow conditions: (a) oxygen volume fraction; (b) coal temperature.

From Figure 7b, with the increase in air flow, the internal temperature of coal is getting higher and higher. Interestingly, the area with a higher temperature in the coal body is located at the inlet of the air. This is because the low-temperature oxidation reaction of coal and oxygen is related to the concentration of oxygen (see Equation (2)). The higher the oxygen, the more intense the coal oxidation reaction. Due to the influence of thermal buoyancy and air flow, the temperature in the coal body shows an ellipse, the center of the high-temperature area is upward, as shown in the example of 144 mL/min.

3.3. Effect of Heating Rate on Coal Spontaneous Combustion Characteristics

The thermal environment outside the coal body also has a great influence on the coal spontaneous combustion process. Therefore, the effect of heating rate on coal spontaneous combustion characteristics is investigated by numerical simulation. The heating rate is taken as a variable and the air supply for programmed heating is controlled to 120 mL/min. Figure 8 presents the outlet oxygen volume fraction and its change rate under different heating rates. It can be seen from Figure 8a that with the increase in heating rate, the decrease in oxygen volume fraction at the outlet is intensifying. The oxygen volume fraction at a heating rate of 0 °C/min has little change with time, which is 20.63% at 10 h, but it is only 0.16% when the heating rate is 0.45 °C/min. Moreover, from Figure 8b that with the increase in heating rate, the peak value of the change rate of oxygen volume fraction increases, it is characterized by “early appearance”, that is, the higher the heating rate, the earlier the peak of oxygen volume fraction change rate appears, which indicates that increasing the heating rate will promote the low-temperature oxidation intensity of coal. This is mainly because coal spontaneous combustion is originally an oxidative exothermic process, and the increase in heating rate further reduces the reaction threshold at the low-temperature stage of coal spontaneous combustion, thereby accelerating the oxidation reaction.

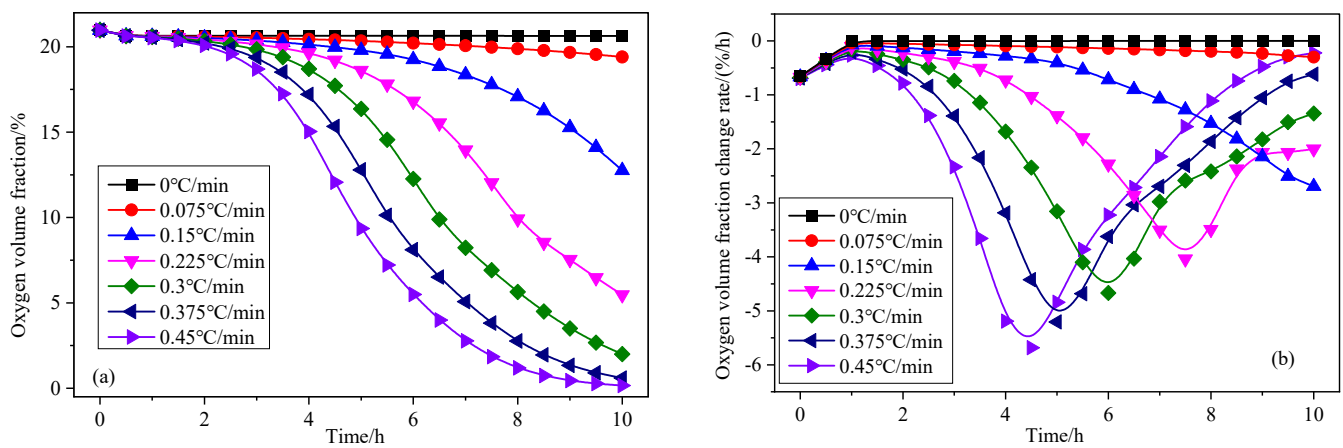


Figure 8. Oxygen volume fraction and its change rate at the outlet under different heating rates: (a) oxygen volume fraction; (b) oxygen volume fraction change rate.

Furthermore, Figure 9 presents the relationship between the peak time of the oxygen volume fraction change rate at the outlet and the heating rate. Since the peak value of outlet oxygen volume fraction change rate corresponding to 0, 0.075, and 0.15 °C/min does not appear within 10 h, only the temperature rise rate greater than 0.225 °C/min is listed. From Figure 9, with the increase in heating rate, the peak time decreases, reflecting the characteristic of “early appearance”, and Equation (8) is obtained by exponential fitting.

$$y = 17.6e^{-x/0.15} + 3.63 \tag{8}$$

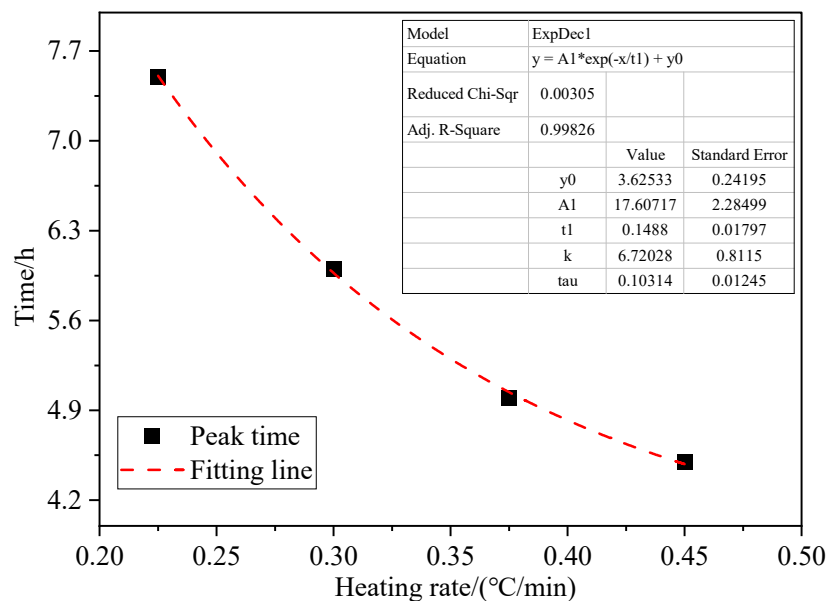


Figure 9. The relationship between the peak time of the outlet oxygen volume fraction change rate and the heating rate.

Figure 10 shows the maximum temperature value and its change rate of coal under different heating rates. On the whole, the higher the heating rate, the faster the temperature rises, indicating that the external thermal environment promotes the coal oxidation process. Meanwhile, except for heating rate 0 °C/min, under other heating conditions, the maximum coal temperature and its change rate always change from lower than the programmed temperature to higher than the programmed temperature, and in the later stage of coal oxidation, the change rate of temperature rise increases and the coal temperature rises faster. This indicates that under the effect of programmed temperature rise, the heat

accumulation of coal low-temperature oxidation exceeds the heat dissipation, and the net heat of coal is positive. Therefore, in the process of prevention and control of coal spontaneous combustion disaster in the mine, the early low-temperature stage is the key to treatment [43]. Once the coal temperature exceeds a certain critical value, usually the dry crack temperature, its oxidation reaction increases rapidly, and spontaneous combustion may occur in a very short time.

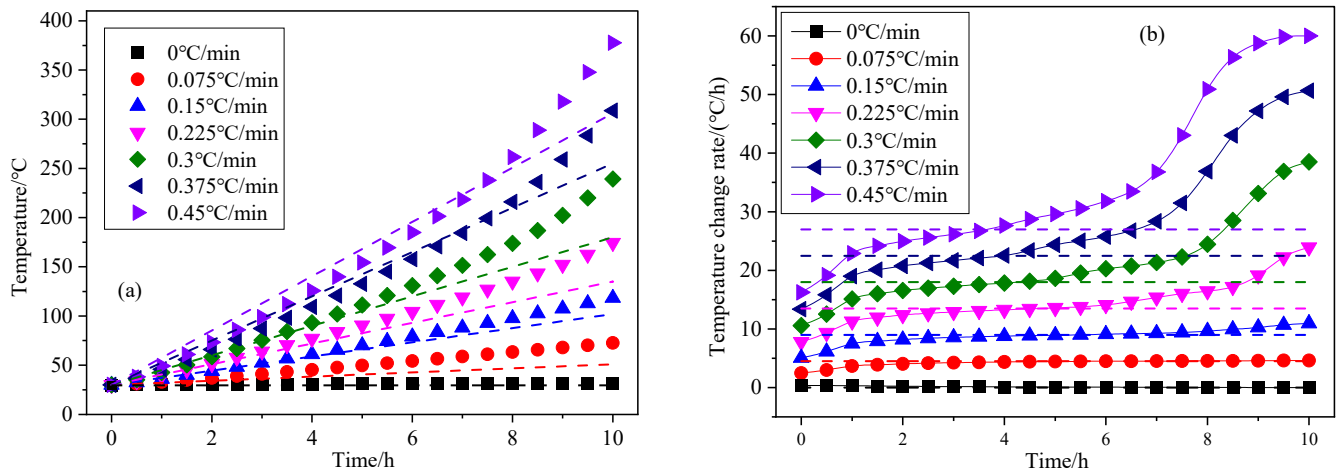


Figure 10. Maximum coal temperature and its change rate under different heating rates: (a) coal temperature; (b) coal temperature change rate.

Figure 11 shows the maximum coal temperature at different heating rates at 10 h. With the increase in heating rate, the maximum coal temperature value presents a linear increase trend, and the linear fitting result is shown in Equation (9). Therefore, in the process of mine production, attention should be paid to controlling the ventilation temperature to prevent it from intensifying the coal oxidation reaction.

$$y = 774.5x + 14 \tag{9}$$

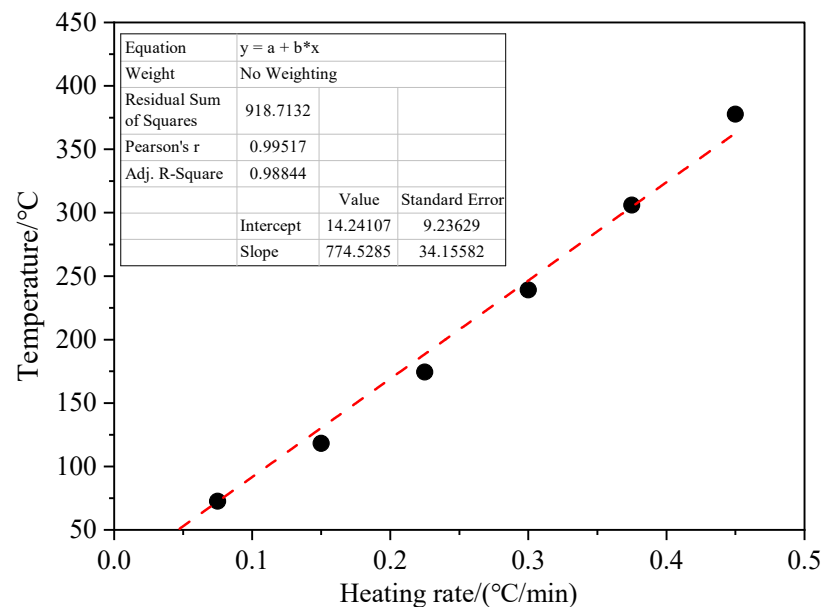


Figure 11. Maximum coal temperature at 10 h under different heating rates.

Figure 12 gives the cloud diagram of oxygen volume fraction and temperature distribution under different heating rate conditions at the 10th hour. According to Figure 12a, the

oxygen volume fraction in the coal storage tank decreases with the increase in the heating rate. As the air enters the coal body from the inlet and then is discharged from the outlet, this process consumes a large amount of oxygen due to the influence of coal oxidation, resulting in the lowest oxygen volume fraction at the outlet. Especially when the heating rate is $0.45\text{ }^{\circ}\text{C}/\text{min}$, the oxygen volume fraction in the coal body is less than 4%, and the higher oxygen volume fraction area is located in the inlet gas buffer zone.

With the increase in heating rate, the coal temperature in the coal storage tank is getting higher and higher, as shown in Figure 12b. The coal temperature distribution corresponding to the heating rate of 0 and $0.15\text{ }^{\circ}\text{C}/\text{min}$ is relatively uniform, which indicates that the oxidation reaction inside the coal is weak under the above conditions, and the change of the coal temperature depends on the external heat transfer. The temperature distribution of coal corresponding to the heating rate of 0.3 and $0.45\text{ }^{\circ}\text{C}/\text{min}$ is uneven, and the high-temperature zone is located at the air inlet. This is because the oxygen volume fraction here is high, which can fully meet the demand of coal oxidation reaction, and the oxidation reaction here is more full and intense. In addition, due to the rapid consumption of oxygen in the coal body at the entrance, the temperature distribution in the upper part of the coal body is characterized by a high surrounding area and low center at the heating rate of 0.3 and $0.45\text{ }^{\circ}\text{C}/\text{min}$. This reflects that under the conditions of heating rates 0.3 and $0.45\text{ }^{\circ}\text{C}/\text{min}$, the temperature of the upper part of the coal body is mainly affected by heat transfer rather than coal oxidation.

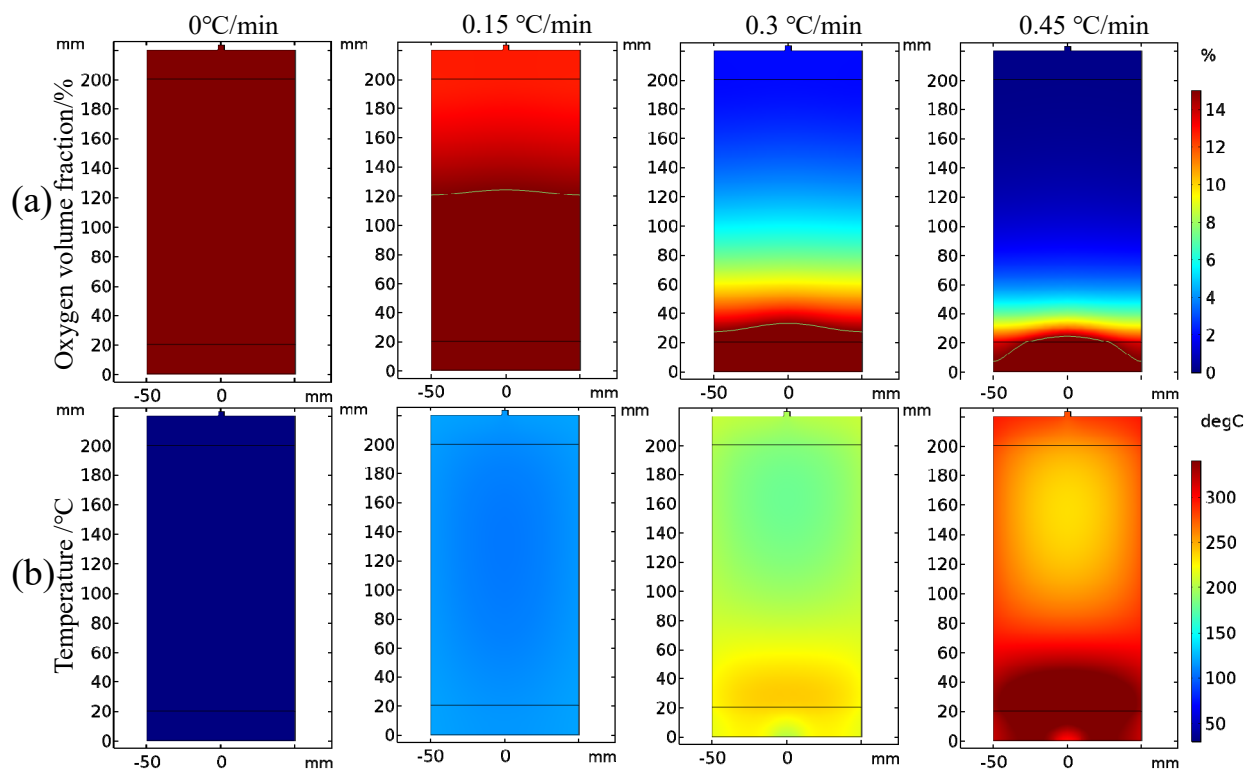


Figure 12. Cloud diagram of oxygen volume fraction and temperature distribution under different heating rates conditions: (a) oxygen volume fraction; (b) coal temperature.

4. Conclusions

- (1) A programmed temperature rise model of coal spontaneous combustion is established using the multi-physical field coupling method to study the characteristics of coal spontaneous combustion under different external air supplies and temperature controls. The average error between simulation results of oxygen and carbon dioxide volume fractions and experimental results is only 2.3% and 4.6%, respectively. The acquisition of numerical simulation parameters and the numerical simulation method

can reasonably characterize the coal oxidation process. The research results have important practical significance for the prevention and control of coal spontaneous combustion in goaf.

- (2) With the increase in air supply volume, the oxygen volume fraction at the outlet increases, and the peak value of the change rate of oxygen volume fraction at the outlet presents the “hysteresis” characteristic. As the air flow increases, the area with high oxygen volume fraction moves upward and the internal temperature of coal is getting higher, and linearly related to the air supply flow. After the air supply flow is greater than 24 mL/min, the maximum coal temperature exceeds the leading temperature of the programmed temperature rise after 7.5 h, its change rate exceeds the programmed temperature rise rate after 4 h, and the oxidation reaction is further intensified.
- (3) As the heating rate increases, the decrease in oxygen volume fraction at the outlet intensifies, and the peak value of the oxygen volume fraction change rate presents the “early appearance” characteristic. The maximum coal temperature and its change rate always change from below the programmed leading temperature (heating rate) to above the programmed leading value, and in the later stage of coal oxidation, their values increase rapidly, and the risk of coal spontaneous combustion also increases further.

Author Contributions: Conceptualization, C.L. and X.S.; methodology, C.L.; software, C.L. and X.S.; validation, L.J., C.D. and J.N.; writing—original draft preparation, C.L.; writing—review and editing, C.L. and X.S.; visualization, C.L.; supervision, C.D. and Y.G.; funding acquisition, C.L. All authors have read and agreed to the published version of the manuscript.

Funding: This research was funded by the National Natural Science Foundation of China, grant numbers 52204229 and 52274220; the Basic Research Program in Shanxi province, grant number 20210302124349; and the Scientific and Technological Innovation Programs of Higher Education Institutions in Shanxi, grant number 2021L054.

Institutional Review Board Statement: Not applicable.

Informed Consent Statement: Not applicable.

Data Availability Statement: Not applicable.

Conflicts of Interest: The authors declare no conflict of interest.

References

1. Ma, T.; Zhai, X.; Xiao, Y.; Bai, Y.; Shen, K.; Song, B.; Hao, L.; Ren, L.; Chen, X. Study on the influence of key active groups on gas products in spontaneous combustion of coal. *Fuel* **2023**, *344*, 128020. [[CrossRef](#)]
2. Li, D.; Wang, E.; Kong, X.; Ali, M.; Wang, D. Mechanical behaviors and acoustic emission fractal characteristics of coal specimens with a pre-existing flaw of various inclinations under uniaxial compression. *Int. J. Rock Mech. Min.* **2019**, *116*, 38–51. [[CrossRef](#)]
3. Xu, K.; Li, S.; Liu, J.; Lu, C.; Xue, G.; Xu, Z.; He, C. Evaluation cloud model of spontaneous combustion fire risk in coal mines by fusing interval gray number and DEMATEL. *Sustainability* **2022**, *14*, 15585. [[CrossRef](#)]
4. Shi, X.; Zhang, Y.; Chen, X.; Zhang, Y.; Rui, L.; Guo, R.; Zhao, T.; Deng, Y. Numerical simulation on response characteristics of coal ignition under the disturbance of fluctuating heat. *Combust. Flame* **2022**, *237*, 111870. [[CrossRef](#)]
5. Ren, S.; Ma, T.; Zhang, Y.; Deng, J.; Xiao, Y.; Zhai, X.; Zhang, Y.; Song, Z.; Wang, C. Sound absorption characteristics of loose bituminous coal porous media with different metamorphic degrees. *Fuel* **2023**, *332*, 126091. [[CrossRef](#)]
6. Kong, X.; He, D.; Liu, X.; Wang, E.; Li, S.; Liu, T.; Ji, P.; Deng, D.; Yang, S. Strain characteristics and energy dissipation laws of gas-bearing coal during impact fracture process. *Energy* **2022**, *242*, 123028. [[CrossRef](#)]
7. Liang, Y.; Zhang, J.; Wang, L.; Luo, H.; Ren, T. Forecasting spontaneous combustion of coal in underground coal mines by index gases: A review. *J. Loss Prev. Proc.* **2019**, *57*, 208–222. [[CrossRef](#)]
8. Sahu, A.K.; Joshi, K.A.; Raghavan, V.; Rangwala, A.S. Comprehensive numerical modeling of ignition of coal dust layers in different configurations. *Proc. Combust. Inst.* **2015**, *35*, 2355–2362. [[CrossRef](#)]
9. Zeneli, M.; Nikolopoulos, A.; Nikolopoulos, N.; Grammelis, P.; Karellas, S.; Kakaras, E. Simulation of the reacting flow within a pilot scale calciner by means of a three phase TFM model. *Fuel Process. Technol.* **2017**, *162*, 105–125. [[CrossRef](#)]
10. Joshi, K.A.; Raghavan, V.; Rangwala, A.S. An experimental study of coal dust ignition in wedge shaped hot plate configurations. *Combust. Flame* **2012**, *159*, 376–384. [[CrossRef](#)]

11. Zhang, Y.; Yang, C.; Li, Y.; Huang, Y.; Zhang, J.; Zhang, Y.; Li, Q. Ultrasonic extraction and oxidation characteristics of functional groups during coal spontaneous combustion. *Fuel* **2019**, *242*, 287–294. [[CrossRef](#)]
12. Zhao, J.; Deng, J.; Wang, T.; Song, J.; Zhang, Y.; Shu, C.; Zeng, Q. Assessing the effectiveness of a high-temperature-programmed experimental system for simulating the spontaneous combustion properties of bituminous coal through thermokinetic analysis of four oxidation stages. *Energy* **2019**, *169*, 587–596. [[CrossRef](#)]
13. Deng, J.; Xiao, Y.; Li, Q.; Lu, J.; Wen, H. Experimental studies of spontaneous combustion and anaerobic cooling of coal. *Fuel* **2015**, *157*, 261–269. [[CrossRef](#)]
14. Qi, G.; Lu, W.; Qi, X.; Zhong, X.; Cheng, W.; Liu, F. Differences in smoldering characteristics of coal piles with different smoldering propagation directions. *Fire Safety J.* **2018**, *102*, 77–82.
15. Wen, H.; Wang, H.; Liu, W.; Cheng, X. Comparative study of experimental testing methods for characterization parameters of coal spontaneous combustion. *Fuel* **2020**, *275*, 117880. [[CrossRef](#)]
16. Beamish, B.B.; Theiler, J. Coal spontaneous combustion: Examples of the self-heating incubation process. *Int. J. Coal Geol.* **2019**, *215*, 103297. [[CrossRef](#)]
17. Zhang, D.; Yang, X.; Deng, J.; Wen, H.; Xiao, Y.; Jia, H. Research on coal spontaneous combustion period based on pure oxygen adiabatic oxidation experiment. *Fuel* **2021**, *288*, 119651. [[CrossRef](#)]
18. Jia, X.; Wu, J.; Lian, C.; Rao, J. Assessment of coal spontaneous combustion index gas under different oxygen concentration environment: An experimental study. *Environ. Sci. Pollut. Res.* **2022**, *29*, 87257–87267. [[CrossRef](#)]
19. Shi, X.; Chen, X.; Zhang, Y.; Zhang, Y.; Guo, R.; Zhao, T.; Liu, R. Numerical simulation of coal dust self-ignition and combustion under inclination conditions. *Energy* **2022**, *239*, 122227. [[CrossRef](#)]
20. Tang, Y.; Zhong, X.; Li, G.; Yang, Z.; Shi, G. Simulation of dynamic temperature evolution in an underground coal fire area based on an optimised Thermal-Hydraulic-Chemical model. *Combust. Theory Model.* **2019**, *23*, 127–146. [[CrossRef](#)]
21. Chen, X.; Shi, X.; Zhang, Y.; Zhang, Y.; Ma, Q. Numerical simulation study on coal spontaneous combustion: Effect of porosity distribution. *Combust. Sci. Technol.* **2023**, *195*, 472–493. [[CrossRef](#)]
22. Wen, H.; Yu, Z.; Deng, J.; Zhai, X. Spontaneous ignition characteristics of coal in a large-scale furnace: An experimental and numerical investigation. *Appl. Therm. Eng.* **2017**, *114*, 583–592. [[CrossRef](#)]
23. Shi, X.; Zhang, Y.; Chen, X.; Zhang, Y. Effects of thermal boundary conditions on spontaneous combustion of coal under temperature-programmed conditions. *Fuel* **2021**, *295*, 120591. [[CrossRef](#)]
24. Li, Z.; Xu, Y.; Liu, H.; Zhai, X.; Zhao, S.; Yu, Z. Numerical analysis on the potential danger zone of compound hazard in gob under mining condition. *Process. Saf. Environ.* **2021**, *147*, 1125–1134. [[CrossRef](#)]
25. Ma, L.; Guo, R.; Wu, M.; Wang, W.; Ren, L.; Wei, G. Determination on the hazard zone of spontaneous coal combustion in the adjacent gob of different mining stages. *Process. Saf. Environ.* **2020**, *142*, 370–379. [[CrossRef](#)]
26. Yuan, L.; Smith, A.C. Numerical study on effects of coal properties on spontaneous heating in longwall gob areas. *Fuel* **2008**, *87*, 3409–3419. [[CrossRef](#)]
27. Liu, W.; Qin, Y.; Shi, C.; Guo, D. Dynamic evolution of spontaneous combustion of coal in longwall gobs during mining-stopped period. *Process. Saf. Environ.* **2019**, *132*, 11–21. [[CrossRef](#)]
28. Ren, L.; Deng, J.; Li, Q.; Ma, L.; Zou, L.; Laiwang, B.; Shu, C. Low-temperature exothermic oxidation characteristics and spontaneous combustion risk of pulverised coal. *Fuel* **2019**, *252*, 238–245. [[CrossRef](#)]
29. Yan, H.; Nie, B.; Liu, P.; Chen, Z.; Yin, F.; Gong, J.; Lin, S.; Wang, X.; Kong, F.; Hou, Y. Experimental investigation and evaluation of influence of oxygen concentration on characteristic parameters of coal spontaneous combustion. *Thermochim. Acta* **2022**, *717*, 179345. [[CrossRef](#)]
30. Zhang, Y.; Zhang, Y.; Li, Y.; Shi, X.; Che, B. Determination of ignition temperature and kinetics and thermodynamics analysis of high-volatile coal based on differential derivative thermogravimetry. *Energy* **2022**, *240*, 122493. [[CrossRef](#)]
31. Sabat, G.; Gouda, N.; Panda, A.K. Effect of coal grade and heating rate on the thermal degradation behavior, kinetics, and thermodynamics of pyrolysis of low-rank coal. *Int. J. Coal Prep. Util.* **2022**, 1–19. [[CrossRef](#)]
32. Wang, Z.; Xu, M.; Fu, X.; Cao, J.; Li, C.; Feng, M.; Li, K. Study on pyrolysis characteristics and kinetics of bituminous coal by thermogravimetric method. *Combust. Sci. Technol.* **2022**, *194*, 558–573. [[CrossRef](#)]
33. Ejlali, A.; Mee, D.J.; Hooman, K.; Beamish, B.B. Numerical modelling of the self-heating process of a wet porous medium. *Int. J. Heat Mass Transf.* **2011**, *54*, 5200–5206. [[CrossRef](#)]
34. Xia, T.; Zhou, F.; Wang, X.; Zhang, Y.; Li, Y.; Kang, J.; Liu, J. Controlling factors of symbiotic disaster between coal gas and spontaneous combustion in longwall mining gobs. *Fuel* **2016**, *182*, 886–896. [[CrossRef](#)]
35. Zheng, Y.; Li, Q.; Zhu, P.; Li, X.; Zhang, G.; Ma, X.; Zhao, Y. Study on multi-field evolution and influencing factors of coal spontaneous combustion in goaf. *Combust. Sci. Technol.* **2023**, *195*, 247–264. [[CrossRef](#)]
36. Wu, D.; Vanierschot, M.; Verplaetsen, F.; Berghmans, J.; Van den Bulck, E. Numerical study on the ignition behavior of coal dust layers in air and O₂/CO₂ atmospheres. *Appl. Therm. Eng.* **2016**, *109*, 709–717. [[CrossRef](#)]
37. Lei, C.; Deng, J.; Cao, K.; Xiao, Y.; Ma, L.; Wang, W.; Ma, T.; Shu, C. A comparison of random forest and support vector machine approaches to predict coal spontaneous combustion in gob. *Fuel* **2019**, *239*, 297–311. [[CrossRef](#)]
38. Deng, J.; Lei, C.; Xiao, Y.; Cao, K.; Ma, L.; Wang, W.; Laiwang, B. Determination and prediction on “three zones” of coal spontaneous combustion in a gob of fully mechanized caving face. *Fuel* **2018**, *211*, 458–470. [[CrossRef](#)]

39. Zhang, Y.; Shu, P.; Deng, J.; Duan, Z.; Li, L.; Zhang, L. Analysis of oxidation pathways for characteristic groups in coal spontaneous combustion. *Energy* **2022**, *254*, 124211. [[CrossRef](#)]
40. Wang, C.; Deng, Y.; Xiao, Y.; Deng, J.; Shu, C.; Jiang, Z. Gas-heat characteristics and oxidation kinetics of coal spontaneous combustion in heating and decaying processes. *Energy* **2022**, *250*, 123810. [[CrossRef](#)]
41. Lei, C.; Jiang, L.; Bao, R.; Deng, C.; Wang, C. Study on multifield migration and evolution law of the oxidation heating process of coal spontaneous combustion in dynamic goaf. *ACS Omega* **2023**, *8*, 14197–14207. [[CrossRef](#)] [[PubMed](#)]
42. Kong, B.; Li, Z.; Yang, Y.; Liu, Z.; Yan, D. A review on the mechanism, risk evaluation, and prevention of coal spontaneous combustion in China. *Environ. Sci. Pollut. Res.* **2017**, *24*, 23453–23470. [[CrossRef](#)] [[PubMed](#)]
43. Lei, C.; Deng, J.; Cao, K.; Ma, L.; Xiao, Y.; Ren, L. A random forest approach for predicting coal spontaneous combustion. *Fuel* **2018**, *223*, 63–73. [[CrossRef](#)]

Disclaimer/Publisher's Note: The statements, opinions and data contained in all publications are solely those of the individual author(s) and contributor(s) and not of MDPI and/or the editor(s). MDPI and/or the editor(s) disclaim responsibility for any injury to people or property resulting from any ideas, methods, instructions or products referred to in the content.